Hindawi Publishing Corporation
Journal of Nanomaterials
Volume 2014, Article ID 962917, 8 pages
http://dx.doi.org/10.1155/2014/962917

Research Article

Optical Nonlinear Refractive Index of Laser-Ablated Gold Nanoparticles Graphene Oxide Composite

Amir Reza Sadrolhosseini,[1] A. S. M. Noor,[1,2] Nastaran Faraji,[3] Alireza Kharazmi,[3] and Mohd. Adzir Mahdi[1,2]

[1] *Wireless and Photonic Networks Research Centre of Excellence (WiPNET), Faculty of Engineering Universiti Putra Malaysia, Malaysia*
[2] *Department of Computer and Communication Systems Engineering, Faculty of Engineering, Universiti Putra Malaysia (UPM), 43400 Serdang, Malaysia*
[3] *Department of Physics, Faculty of Science, Universiti Putra Malaysia (UPM), 43400 Serdang, Malaysia*

Correspondence should be addressed to Amir Reza Sadrolhosseini; amir1348@gmail.com and A. S. M. Noor; ashukri@upm.edu.my

Received 5 June 2014; Revised 26 August 2014; Accepted 7 September 2014; Published 3 November 2014

Academic Editor: Tianxi Liu

Gold nanoparticles were prepared in graphene oxide using laser ablation technique. The ablation times were varied from 10 to 40 minutes, and the particle size was decreased from 16.55 nm to 5.18 nm in spherical shape. The nanoparticles were capped with carboxyl and the hydroxyl groups were obtained from Fourier transform infrared spectroscopy. Furthermore, the UV-visible peak shifted with decreasing of nanoparticles size, appearing from 528 nm to 510 nm. The Z-scan technique was used to measure the nonlinear refractive indices of graphene oxide with different concentrations and a gold nanoparticle graphene oxide nanocomposite. Consequently, the optical nonlinear refractive indices of graphene oxide and gold nanoparticle graphene oxide nanocomposite were shifted from 1.63×10^{-9} cm^2/W to 4.1×10^{-9} cm^2/W and from 1.85×10^{-9} cm^2/W to 5.8×10^{-9} cm^2/W, respectively.

1. Introduction

In recent years, gold nanoparticles (Au-NPs) raise more applications for electronics [1], photodynamic therapy [2], therapeutic agent delivery [3], sensors [4], and medical diagnoses [5]. The electrical field of light can interact strongly with the gold nanoparticles [4], and they produce surface plasmon absorption in the visible range [6]. The coherent excitation of free electrons causes the surface plasmon band in a colloidal nanoparticle [7]. The response of the nanoparticles to an interaction of light beam depends on particle size, the surrounding material, and nanoparticle concentration [8]. Many methods were presented to prepare the Au-NPs such as chemical methods [9, 10], plane leaf extract [11], microwave method [12], and sonochemical method [13]. The gold nanoparticles were prepared in dimethyl sulfoxide, acetonitrile, tetrahydrofuran [14], and nonorganic liquid [15] using laser ablation.

Graphene oxide (GO) is a single-atomic-layered material derived from graphite oxide crystal. It has the ability to dissolve and disperse in a variety of solutions including water. GO can be used in solar cells [16], medicine, biology [17–19], and inorganic optoelectronic devices [20]. The GO molecular structure includes hydroxyl (OH^-) and epoxy ($-COO^-$) groups at the basal plane and carboxyl groups ($-COO^-$) at the edge of the molecular structure [21, 22].

The Z-scan is a versatile technique used to measure the nonlinear refractive index of the nanocomposite. This method is based on inducing a lens inside the sample due to the intensity of a laser beam. The intensity of the laser beam is a function of the focus position, and the variations of intensity should be registered. In this work, the Au-NPs were decorated in GO using laser ablation. The samples were characterized using transmission electron microscopy (TEM), UV-visible and Fourier transformed infrared spectroscopy (FT-IR), atomic absorption spectroscopy (AAA), and Z-scan.

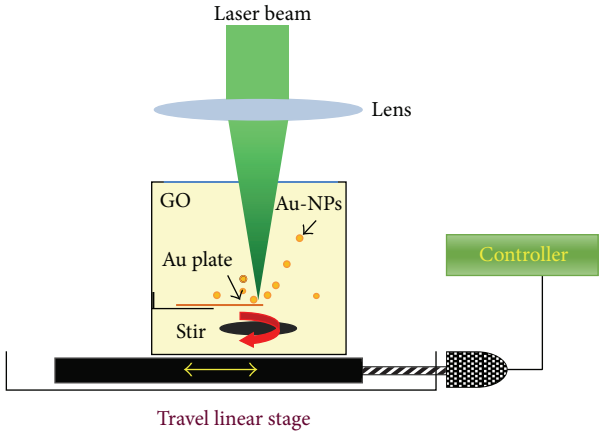

Figure 1: Laser ablation setup for fabrication of Au-NPs in the GO. The position of laser beam and lens are constant. During the ablation of gold plate, the solution container was moved to provide the fresh surface using travel linear stage.

2. Experiment

2.1. Preparation of Graphene Oxide. In 2011, Huang et al. [23] reported the preparation of graphene oxide. Briefly, the graphene oxide was produced with oxidation of graphite. In this process, $H_2SO_4 : H_3PO_4$ (320 : 80 mL), graphite splinter, and $KMnO_4$ (18 g) were mixed using a magnetic stirrer for 3 days to form the GO; the color of the mixture changed to dark brown. Afterward, the H_2O_2 solution was added to stop the oxidation process. The graphite oxide that formed was washed three times with 1 M of HCl aqueous solution and repeatedly with deionized water until a pH of 4-5 was achieved. The washing process was carried out using a simple decantation of supernatant via a centrifugation technique having a centrifugation force of 10,000 g. During the washing process using deionized water, the graphite oxide experienced exfoliation, which resulted in a thickening of the graphene solution, forming a GO gel. The final concentration of GO was 2 mg/mL, and for this experiment, the final solution was dissolved systemically in deionized water, achieving 0.1, 0.3, 0.5, and 0.8 mg/mL.

2.2. Laser Ablation Synthesis of Gold Nanoparticle. In this experiment, a gold plate (Aldrich, high impurity 99.99%) was immersed in 10 mL of GO with a concentration about 0.1 mg/mL. A laser beam of 532 nm wavelength with duration of 10 ns and 1200 mJ has ablated the gold plate in different times with 40 Hz repetition rate. Figure 1 shows the laser ablation setup which contains a Q-switched Nd:YAG laser, a solution container, a gold plate, a lens ($f = 30$ cm), a travel linear stage (New port, IMS Series), and a stirrer. The gold nanoparticle formed in the GO solution during laser ablation of the gold plate with ablation times of 10, 20, 30, and 40 minutes. In order to make sure that the gold nanoparticles disperse evenly in the GO solution, stirring of the solution was performed during the ablation of gold plate, and the solution container moved horizontally using travel linear stage for providing the fresh surface to ablate the target.

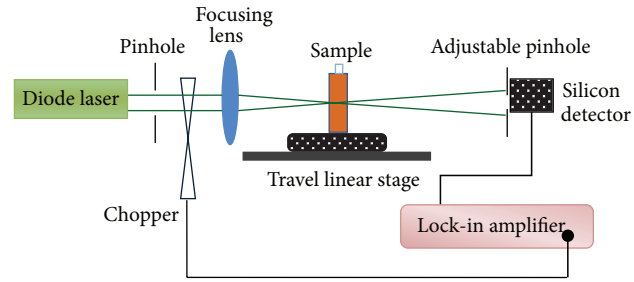

Figure 2: Z-scan setup for measuring the nonlinear refractive index. The adjustable pinhole size is 2 mm.

The UV-visible spectrum, morphology, size, and concentration of the prepared samples were obtained with the UV-visible double-beam spectrophotometer (Shimadzu), transmission electron microscopy (TEM, Hitachi H-7100; Hitachi, Chula Vista, CA), Fourier transform infrared spectroscopy (FT-IR), and atomic absorption spectroscopy (AAS, S series), respectively. The nonlinear refractive indices of GO with different concentrations and Au-NPs/GO nanocomposite were measured using Z-scan technique.

2.3. Z-scan Setup. The Z-scan setup is shown in Figure 2. The setup consists of a diode laser (532 nm, 180 mW), a pinhole, a lens, a travel linear stage (New port, IMS Series), a quartz cell (1 mm), a silicon detector, a chopper, a lock in amplifier, and an adjustable pinhole.

This Z-scan setup was used to measure the nonlinear refractive indices of GO and the Au-NPs/GO nanocomposite. The theoretical formula used to explain the nonlinear coefficient was as follows [24]:

$$\Delta T(z) = 1 - \frac{4\Delta\varphi_0 x}{(x^2+1)(x^2+9)}, \quad (1)$$

where x is normalized distance and is related to the movement distance of sample (z) through $x = z/z_0$ and z_0 is the Rayleigh length and $\Delta\phi_0$ is the phase change [25]. The nonlinear refractive index n_2 is related to phase change by [26]

$$n_2 = \frac{\Delta\phi_0}{kL_{\text{eff}}I_0}, \quad (2)$$

where $k = 2\pi/\lambda$ is the wave vector, $L_{\text{eff}} = (1 - \exp(-\alpha_0 L))/\alpha_0$ is the effective length of nonlinear medium, I_0 is the on-axis irradiance at focus, α_0 is the linear absorption coefficient of the samples, and L is the sample thickness. A quartz cell with 1 mm thickness was used in this experiment.

3. Results and Discussion

Figure 3 shows the UV-visible spectrum of GO with the gold nanoparticles. The baseline of the optical absorption spectra was related to the GO pure before ablation of the gold plate. In accordance with Figure 3, the UV-visible peaks appeared at about 528 nm, 525, 518 nm, and 510 nm. These

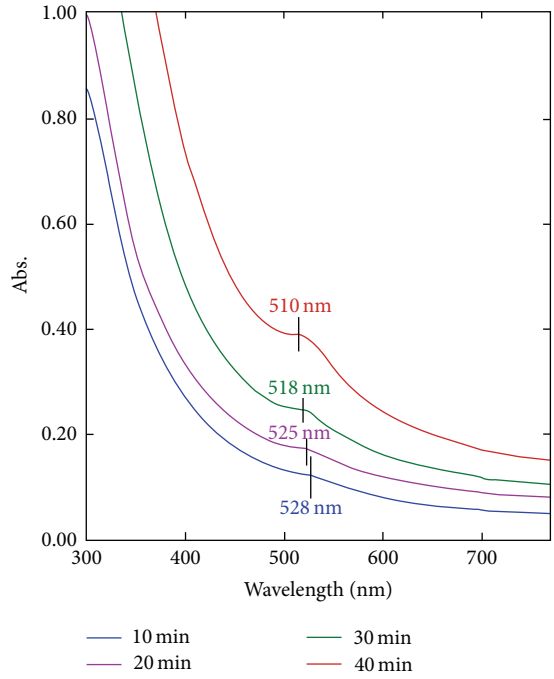

Figure 3: UV-visible spectrum of Au-NPs/GO composite for different ablation times from 10 to 40 minutes.

peaks appear from a localized surface plasmon resonance of Au-NPs. Hence, they confirm that the Au-NPs were formed in GO. The ablation times were 10, 20, 30, and 40 minutes, and the peak intensity of UV-visible spectrum increased with an increase in the ablation time.

Figures 4(a), 4(b), 4(c), and 4(d) show the TEM micrograph. The particle size was obtained via the analysis of the images by the UTHSCSA image tool software program, shown in Figures 4(e), 4(f), 4(g), and 4(h) for the different ablation times. The particle size was decreased from 16.55 nm to 5.18 nm while increasing the ablation time. Figure 4 demonstrates that the particles have a spherical shape, and the distribution of the particles increased with an increase in ablation time.

The FT-IR spectrum was recorded to investigate the chemical structure and the possible boundary of products, as depicted in Figures 5(a) and 5(b) for the GO and Au-NPs/GO composite, respectively, at a frequency range of 4000 to 300 cm^{-1}. The FT-IR peaks are sorted in Table 1. The FT-IR spectrum of the GO was revealed at the C–H stretching vibration at 2925 cm^{-1} and 2856 cm^{-1}, the C–OH stretching peak at 1368 cm^{-1}, the C–O–C stretching peak at 1219 cm^{-1}, and the aromatic C–H peak at 771 cm^{-1}. The FT-IR spectrum of the Au-NPs/GO composites indicated similar peaks. In addition, new peaks at 1458 cm^{-1}, 1163 cm^{-1}, and 455 cm^{-1} corresponded to the OH deformation vibration [27] for C–O stretching and the vibration bands of COOH and the Au-NPs, respectively. Indeed, the appearance of two peaks at 1458 cm^{-1} and 1163 cm^{-1} was due to the strong link of COO^- and OH to the Au-NPs [28, 29]. Hence, the Au-NPs are strongly capped with the COO^- and OH groups for the GO sheets. Figure 5(c) shows the GO sheet before the ablation of gold plate; as mentioned above, the Au-NPs are decorated on the surface and between the GO sheets as shown in Figure 5(d). It is worth mentioning that no impurity was observed in the final products, which was the consequence of the considerable advantages of the laser ablation method.

Table 1: The FT-IR peaks for GO and Au-NPs/GO nanocomposite.

GO	Au-NPs/GO	Definition of peaks
—	455	Au-NPs
771	772	Aromatic C–H
—	1163	Vibration band of COOH
1219	1221	C–O–C stretching
1368	1374	C–OH stretching
—	1458	OH deformation vibration of C–O stretching
2856	2856	C–H stretching vibration
2925	2925	C–H stretching vibration

Table 2: The nonlinear refractive index of the GO with different concentrations. The accuracy of refractive index was calculated from $\delta n_0 = n_2 \times \delta(\Delta\phi_0)/\Delta\phi_0$.

Concentration (mg/mL)	$\lvert\Delta\varphi_0\rvert$ ($\delta(\Delta\phi_0) = 0.02$)	$n_2 \times 10^{-9}$ (cm^2/W)
0.1	1.2	-1.63 ± 0.032
0.3	2.1	-2.15 ± 0.043
0.5	4.2	-3.32 ± 0.06
0.8	5.4	-4.1 ± 0.08

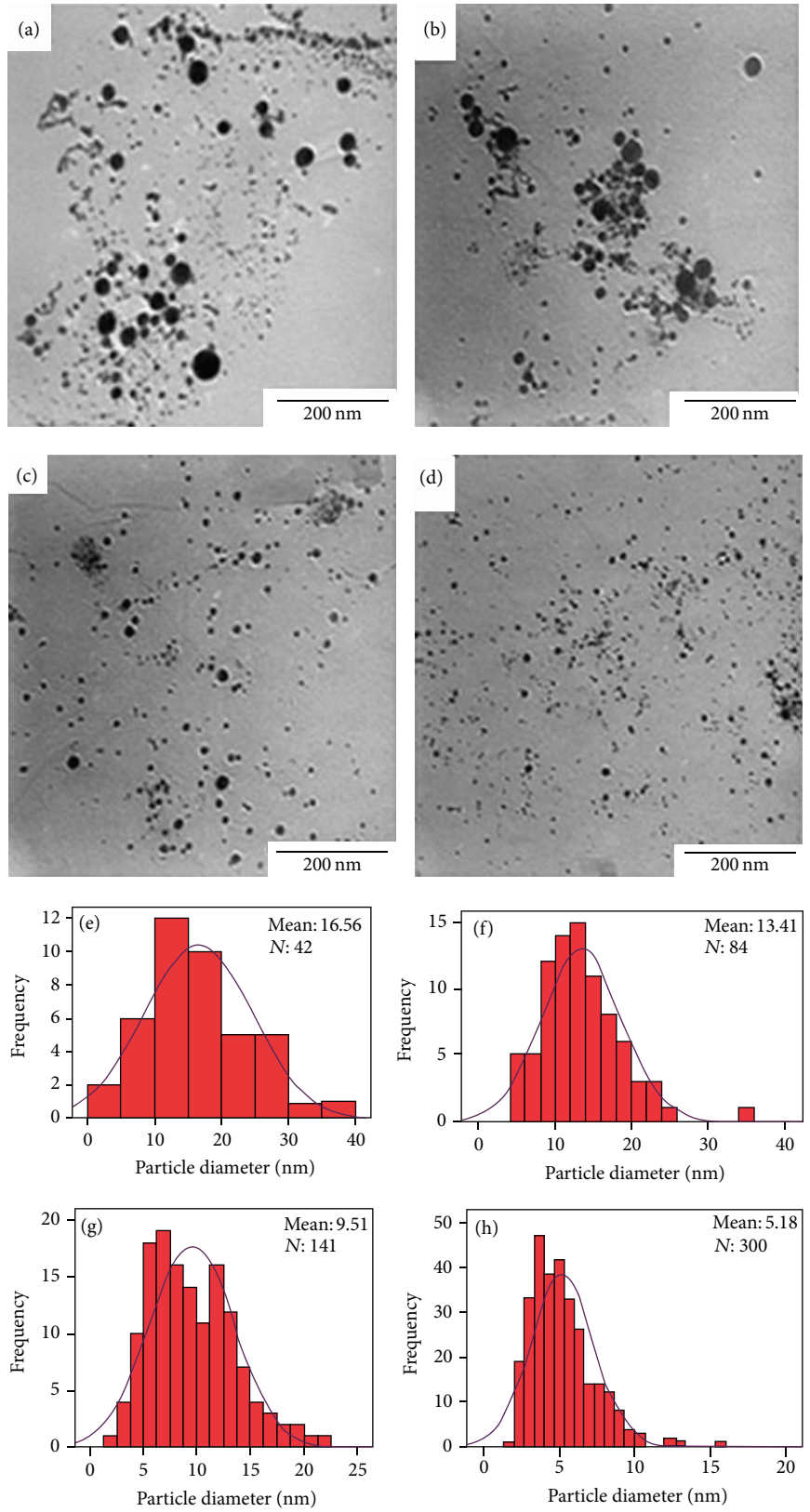

Figure 4: Transmission electron microscopy (TEM) patterns show the particles shape are spherical and the particle sizes for 10, 20, 30, and 40 minutes are 16.55 nm ((a) and (e)), 13.4 nm ((b) and (f)), 9.51 nm ((c) and (g)), and 5.18 nm ((d) and(h)), respectively.

Table 3: Pertinent parameters of the Au-NPs/GO nanocomposite.

Sample	Concentration (ppm)	Size (nm)	Volume fraction (10^{-6})	$\lvert\Delta\varphi_0\rvert$ ($\delta(\Delta\phi_0) = 0.02$)	$n_2 \times 10^{-9}$ (cm^2/W)
10 min	1.2	16.55	0.0580	4.5	-1.85 ± 0.037
20 min	3.21	13.41	0.1663	4.8	-2.7 ± 0.054
30 min	5.79	9.52	0.2995	5.3	-4.1 ± 0.082
40 min	8.41	5.18	0.4358	5.6	-5.8 ± 0.116

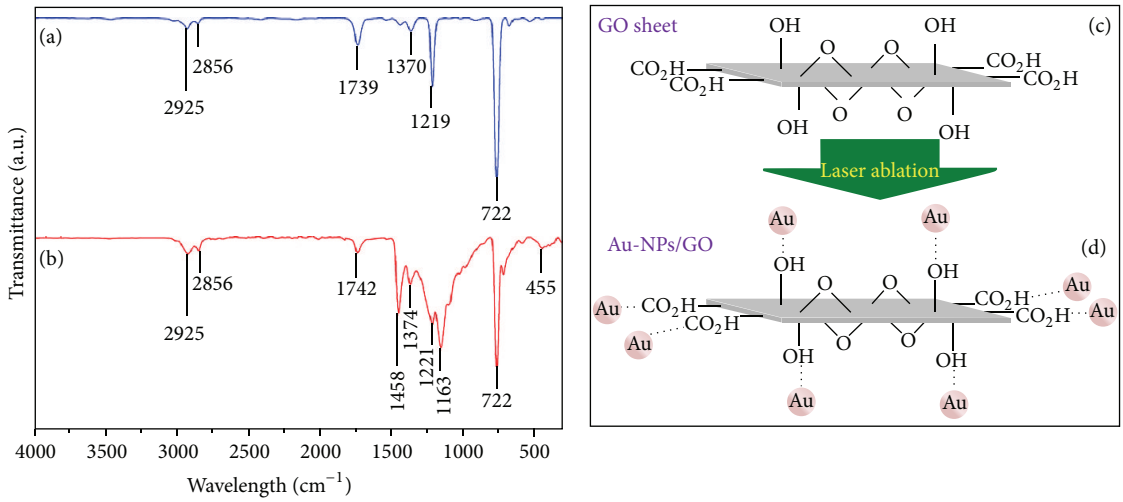

Figure 5: FT-IR spectrum for (a) GO, (b) Au-NPs/GO nanocomposite, (c) GO sheet before the ablation of gold plate, and (d) GO sheet after the ablation of gold target and it shows the Au-NPs decorated the GO sheet.

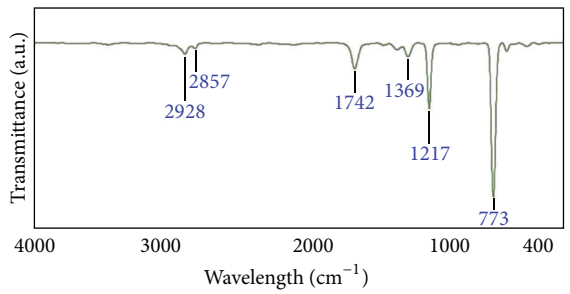

Figure 6: FT-IR results related to pure GO after the irradiation of laser without target plate.

Moreover, Figure 6 illuminates the FT-IR result related to pure GO after the irradiation of laser at 40 minutes without gold plate. The main peaks appear at 2928 cm^{-1}, 2857 cm^{-1}, 1742 cm^{-1}, 1369 cm^{-1}, 1217 cm^{-1}, and 773 cm^{-1}. These peaks are much the same peaks of pure GO before (Figure 5(a)) the irradiation of laser. Consequently, the laser beam did not change any band in GO.

The Z-scan experiment was carried out separately to measure the nonlinear refractive index of pure GO and the Au-NPs/GO nanocomposite. The travel linear stage was moved up to 30 mm with increment of distance of about 0.1 mm. The experiment was repeated for different concentrations of GO from 0.1 mg/mL to 0.8 mg/mL; the transmittance of the Z-scan test versus variation of distance around the focal length is depicted in Figure 7, and $\Delta\varphi_0$ the phase change was obtained after fitting (1) to experiment with 0.02 limit. The nonlinear refractive index of GO was obtained from (2) with average limitation of about 0.056 for each concentration of the GO, while the refractive index was shifted from 1.63×10^{-9} cm^2/W to 4.1×10^{-9} cm^2/W (see Table 2).

The Au-NPs were dispersed in the GO with a 0.1 mg/mL concentration using the laser ablation technique. The ablation times were 10, 20, 30, and 40 minutes, and the theoretical formula (1) was fitted to the experimental data. Afterward,

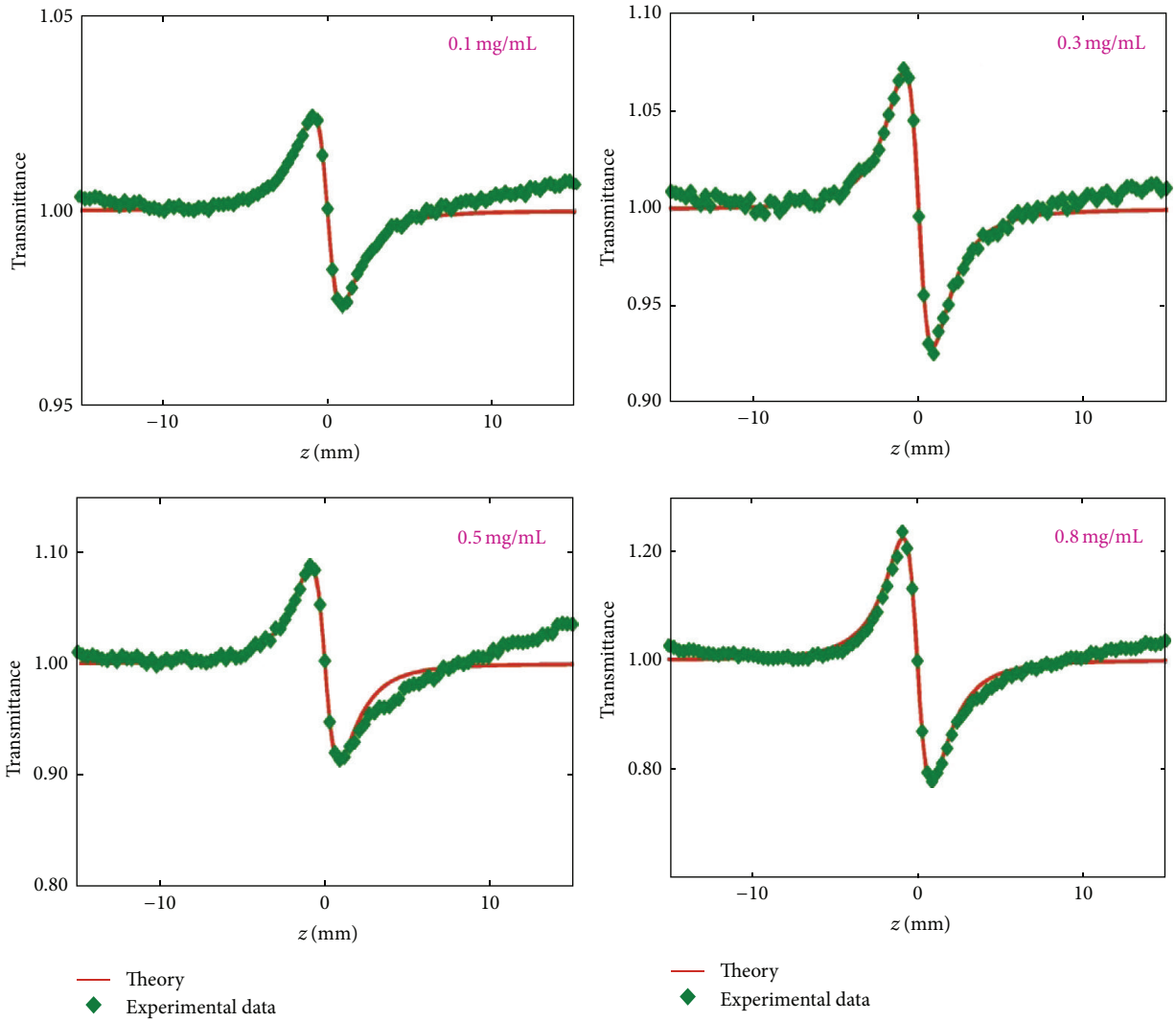

Figure 7: Z-scan transmittance plot for the GO solution for different concentrations of the GO in water.

the nonlinear refractive index for each sample was obtained by calculating (2) with average limitation about 0.07. The transmittance Z-scan signals at the presence of Au-NPs are shown in Figure 8 and the pertinent parameters are sorted in Table 3. Consequently, the nonlinear refractive index of the GO is increasing by increasing the concentration of the GO in solvent. The GO solution and the Au-NPs/GO nanocomposite showed self-defocusing behavior because the refractive index signs were negative.

The concentration of Au-NPs in the GO was measured using AAS. It increased from 1.2 to 8.41 mg/L, and the volume fraction [30] of the gold nanoparticles increased from 0.058×10^{-6} to 0.4358×10^{-6} (Table 3). The nonlinear refractive indices increased by increasing the concentration of the GO and the volume fraction for the Au-NPs. Moreover, the nonlinear refractive index of Au-NPs/GO is larger than the GO-free NPs at the same concentration and increases when increasing the volume fraction of the nanofluid (see Figure 9).

4. Conclusion

The gold nanoparticles were synthesized in the GO using the laser ablation method. The hydroxyl and carboxyl groups of the GO capped the Au-NPs in the edge and between the GO sheets. The particles size of 16.55 nm, 13.41 nm, 9.51 nm, and 5.18 nm were obtained for 10, 20, 30, and 40 minutes of ablation times, respectively; hence, the blue shift appeared in UV-visible spectrum. Consequently, the particles size was reduced, and the absorption and volume fraction were increased. Au-NPs remained completely stable for a long time and distributed homogeneously in the GO. The optical nonlinear refractive index of the GO and Au-NPs GO nanocomposite increased when increasing the concentration of the GO and Au-NPs.

Conflict of Interests

The authors declare that there is no conflict of interests regarding the publication of this paper.

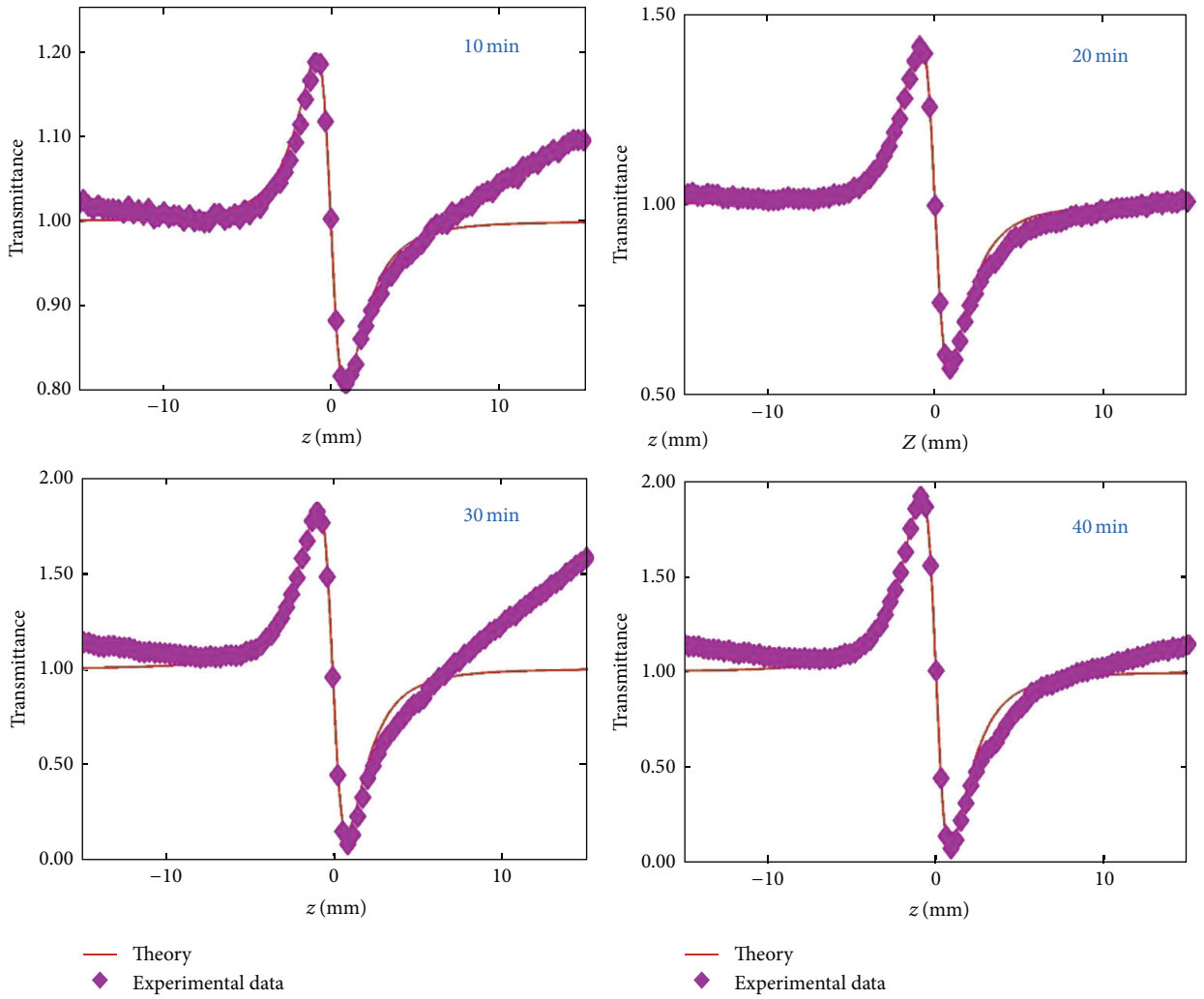

Figure 8: Z-scan transmittance plot for the Au-NPs/GO nanocomposite for different ablation times.

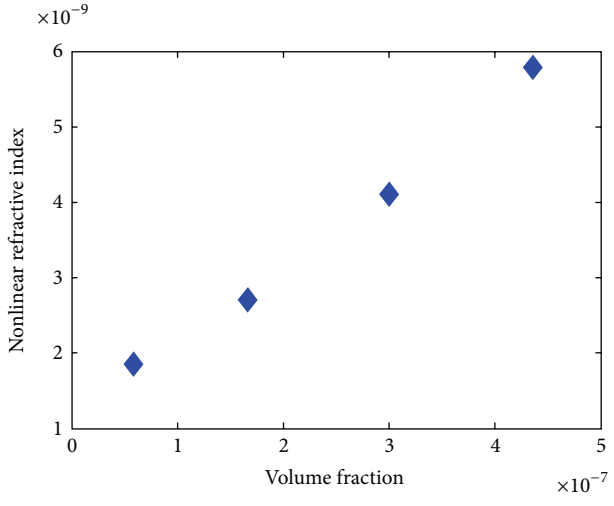

Figure 9: The variation of nonlinear refractive indices of nanocomposite versus volume fraction.

Acknowledgments

The authors acknowledge Universiti Putra Malaysia for the fund from the Research University Grant Scheme (05-02-12-2015RU/05-01-12-1626RU/05-01-12-1627RU/05-02-12-2198RU) and the postdoctoral fellowship under the Wireless and Photonics Network Research Centre (WiPNET).

References

[1] A. Tomar and G. Garg, "Short review on application of gold nanoparticles," *Global Journal of Pharmacology*, vol. 7, no. 1, pp. 34–38, 2013.

[2] M. K. Khaing Oo, Y. Yang, Y. Hu, M. Gomez, H. Du, and H. Wang, "Gold nanoparticle-enhanced and size-dependent generation of reactive oxygen species from protoporphyrin IX," *ACS Nano*, vol. 6, no. 3, pp. 1939–1947, 2012.

[3] L. Vigderman and E. R. Zubarev, "Therapeutic platforms based on gold nanoparticles and their covalent conjugates with drug molecules," *Advanced Drug Delivery Reviews*, vol. 65, no. 5, pp. 663–676, 2013.

[4] K. Saha, S. S. Agasti, C. Kim, X. Li, and V. M. Rotello, "Gold nanoparticles in chemical and biological sensing," *Chemical Reviews*, vol. 112, no. 5, pp. 2739–2779, 2012.

[5] W. Cai, T. Gao, H. Hong, and J. Sun, "Applications of gold nanoparticles in cancer nanotechnology," *Nanotechnology, Science and Applications*, vol. 1, pp. 17–32, 2008.

[6] N. J. Halas, S. Lal, W.-S. Chang, S. Link, and P. Nordlander, "Plasmons in strongly coupled metallic nanostructures," *Chemical Reviews*, vol. 111, no. 6, pp. 3913–3961, 2011.

[7] P. K. Jain, K. S. Lee, I. H. El-Sayed, and M. A. El-Sayed, "Calculated absorption and scattering properties of gold nanoparticles of different size, shape, and composition: applications in biological imaging and biomedicine," *Journal of Physical Chemistry B*, vol. 110, no. 14, pp. 7238–7248, 2006.

[8] A. C. Templeton, J. J. Pietron, R. W. Murray, and P. Mulvaney, "Solvent refractive index and core charge influences on the surface plasmon absorbance of alkanethiolate monolayer-protected gold clusters," *Journal of Physical Chemistry B*, vol. 104, no. 3, pp. 564–570, 2000.

[9] M. Faraday, "The Bakerian lecture: experimental relations of gold (and other metals) to light," *Philosophical Transactions of the Royal Society of London*, vol. 147, pp. 145–181, 1857.

[10] J. Turkevich, P. C. Stevenson, and J. Hillier, "A study of the nucleation and growth processes in the synthesis of colloidal gold," *Discussions of the Faraday Society*, vol. 11, pp. 55–75, 1951.

[11] Y. Li, T.-Y. Wu, S.-M. Chen, M. A. Ali, and F. M. A. AlHemaid, "Green synthesis and electrochemical characterizations of gold nanoparticles using leaf extract of Magnolia kobus," *International Journal of Electrochemical Science*, vol. 7, no. 12, pp. 12742–12751, 2012.

[12] R. Das, P. J. Babu, N. Gogoi, P. Sharma, and U. Bora, "Microwave-mediated rapid synthesis of gold nanoparticles Using *Calotropis procera* latex and study of optical properties," *ISRN Nanomaterials*, vol. 2012, Article ID 650759, 6 pages, 2012.

[13] K. Okitsu, M. Ashokkumar, and F. Grieser, "Sonochemical synthesis of gold nanoparticles: effects of ultrasound frequency," *Journal of Physical Chemistry B*, vol. 109, no. 44, pp. 20673–20675, 2005.

[14] V. Amendola, S. Polizzi, and M. Meneghetti, "Laser ablation synthesis of gold nanoparticles in organic solvents," *Journal of Physical Chemistry B*, vol. 110, no. 14, pp. 7232–7237, 2006.

[15] E. V. Barmina, G. A. Shafeev, P. G. Kuzmin, A. A. Serkov, A. V. Simakin, and N. N. Melnik, "Laser-assisted generation of gold nanoparticles and nanostructures in liquid and their plasmonic luminescence," *Applied Physics A: Materials Science and Processing*, vol. 115, no. 3, pp. 747–752, 2014.

[16] Y. Zhu, S. Murali, W. Cai et al., "Graphene and graphene oxide: synthesis, properties, and applications," *Advanced Materials*, vol. 22, no. 35, pp. 3906–3924, 2010.

[17] Y. Song, K. Qu, C. Zhao, J. Ren, and X. Qu, "Graphene oxide: intrinsic peroxidase catalytic activity and its application to glucose detection," *Advanced Materials*, vol. 22, no. 19, pp. 2206–2210, 2010.

[18] M. Lv, Y. Zhang, L. Liang et al., "Effect of graphene oxide on undifferentiated and retinoic acid-differentiated SH-SY5Y cells line," *Nanoscale*, vol. 4, no. 13, pp. 3861–3866, 2012.

[19] W. Hu, C. Peng, W. Luo et al., "Graphene-based antibacterial paper," *ACS Nano*, vol. 4, no. 7, pp. 4317–4323, 2010.

[20] M. Choe, C.-Y. Cho, J.-P. Shim et al., "Au nanoparticle-decorated graphene electrodes for GaN-based optoelectronic devices," *Applied Physics Letters*, vol. 101, no. 3, Article ID 031115, 2012.

[21] G. Eda and M. Chhowalla, "Chemically derived graphene oxide: towards large-area thin-film electronics and optoelectronics," *Advanced Materials*, vol. 22, no. 22, pp. 2392–2415, 2010.

[22] D. S. Sutar, G. Singh, and V. D. Botcha, "Electronic structure of graphene oxide and reduced graphene oxide monolayers," *Applied Physics Letters*, vol. 101, no. 10, Article ID 103103, 2012.

[23] N. M. Huang, H. N. Lim, C. H. Chia, M. A. Yarmo, and M. R. Muhamad, "Simple room-temperature preparation of high-yield large-area graphene oxide," *International Journal of Nanomedicine*, vol. 6, pp. 3443–3448, 2011.

[24] A. Granmayeh Rad, H. Abbasi, and K. Golyari, "Fabrication and nonlinear refractive index measurement of colloidal silver nanoparticles," *International Journal of Applied Physics and Mathematics*, vol. 2, no. 2, pp. 135–139, 2012.

[25] M. Sheik-Bahae, A. A. Said, T. H. Wei, D. J. Hagan, and E. W. van Stryland, "Sensitive measurement of optical nonlinearities using a single beam," *IEEE Journal of Quantum Electronics*, vol. 26, no. 4, pp. 760–769, 1990.

[26] M. Sheik-Bahae, A. A. Said, and E. W. van Stryland, "High-sensitivity, single-beam n_2 measurements," *Optics Letters*, vol. 14, no. 27, pp. 95–957, 1989.

[27] S. Ge, M. Yan, J. Lu et al., "Electrochemical biosensor based on graphene oxide–Au nanoclusters composites for l-cysteine analysis," *Biosensors and Bioelectronics*, vol. 31, no. 1, pp. 49–54, 2012.

[28] P.-G. Ren, D.-X. Yan, X. Ji, T. Chen, and Z.-M. Li, "Temperature dependence of grapheme oxide reduced by hydrazine hydrate," *Nanotechnology*, vol. 22, no. 5, Article ID 055705, 2011.

[29] Z. Niu, J. Chen, H. H. Hng, J. Ma, and X. Chen, "A leavening strategy to prepare reduced graphene oxide foams," *Advanced Materials*, vol. 24, no. 30, pp. 4144–4150, 2012.

[30] A. R. Sadrolhosseini, A. S. Noor, K. Shameli, G. Mamdoohi, M. M. Moksin, and M. Adzir Mahdi, "Laser ablation synthesis and optical properties of copper nanoparticles," *Journal of Materials Research*, vol. 28, no. 18, pp. 2629–2636, 2013.